Electrochemical Science Advances

WILEY-VCH

ELECTROCHEMICAL SCIENCE ADVANCES Open Access

Perspective OPEN ACCESS

Connecting Cell Structure and Current-Dependent Environment Changes in CO_2 Electrolysis to GDE Operation Regimes and Multi-Cell Interaction

Christina Martens[1,2] | Maximilian Quentmeier[1,2] | Bernhard Schmid[1] | Hermann Tempel[1] | Rüdiger-A. Eichel[1,2]

[1]Institute of Energy Technologies–Fundamental Electrochemistry (IET-1), Forschungszentrum Jülich GmbH, Jülich, Germany | [2]Institute of Physical Chemistry, RWTH Aachen University, Aachen, Germany

Correspondence: Christina Martens (c.martens@fz-juelich.de) | Bernhard Schmid (b.schmid@fz-juelich.de)

Received: 5 June 2024 | **Revised:** 17 July 2024 | **Accepted:** 27 July 2024

Funding: This research was supported by the German Federal Ministry of Education and Research (BMBF) within the project iNEW2.0 – Inkubator Nachhaltige Elektrochemie (03SF0627A).

ABSTRACT

Consecutive development of materials, components, and ultimately, devices does not appear to be a promising strategy in CO_2 electroreduction because maintaining comparability and transferring results between idealized and application-oriented systems proves challenging. A modular cell design and tracking cell conditions *via* sensors may be a solution. We displayed a strategy to characterize gas diffusion electrode operating regimes in a flow cell with regard to different current density ranges, as well as the impact of the flow gap design. We revealed strong interdependencies between cell components, their functions as well as individual cells when integrated into a stack. Expanding the scope and resolution of experimental data made new information on the change of system parameters in flow cells accessible.

1 | Introduction

Research into technologies such as aqueous CO_2 reduction, which may provide green chemicals under benign operating conditions, needs to be efficient and fast. This is especially challenging when dealing with an electrochemical reaction taking place on a solid electrode involving gaseous educts and products and an amphoteric liquid environment [1]. Overcoming the challenges of this reaction requires focusing on specific questions while keeping the other variables constant. Rapid progress can be achieved when developments are conducted in parallel whenever stable reference systems are available. Development of gas diffusion electrodes (GDEs) [2, 3], for instance, was extensively conducted using the selective and stable CO-producing catalyst Ag, while catalyst research on the hydrocarbon-producing catalyst Cu is still ongoing, using solid electrodes in static electrolytes to ensure stable reference conditions (H-cells) [4]. Recently, the stability of GDEs and membranes has improved to the point where they can be used as a stable reference [5, 6] to elucidate questions regarding the full cell [7], such as the interdependence of the conditions in the cell and the GDE performance or the effects of stacking multiple cells in series with shared electrolyte and educt supply [8].

2 | Determining the Scope of Valid Performance Indicators and Influence Factors by Experiment Design

GDEs are widely considered the key component to achieving application-relevant current densities in electrochemical CO_2 reduction and contain the electrocatalyst [2, 9]. Hence,

The first three authors have contributed equally to the paper and share the position of the first author. All three authors have the right to put their names in the first position in their resume and publication records. The author names on the publication are in alphabetical order.

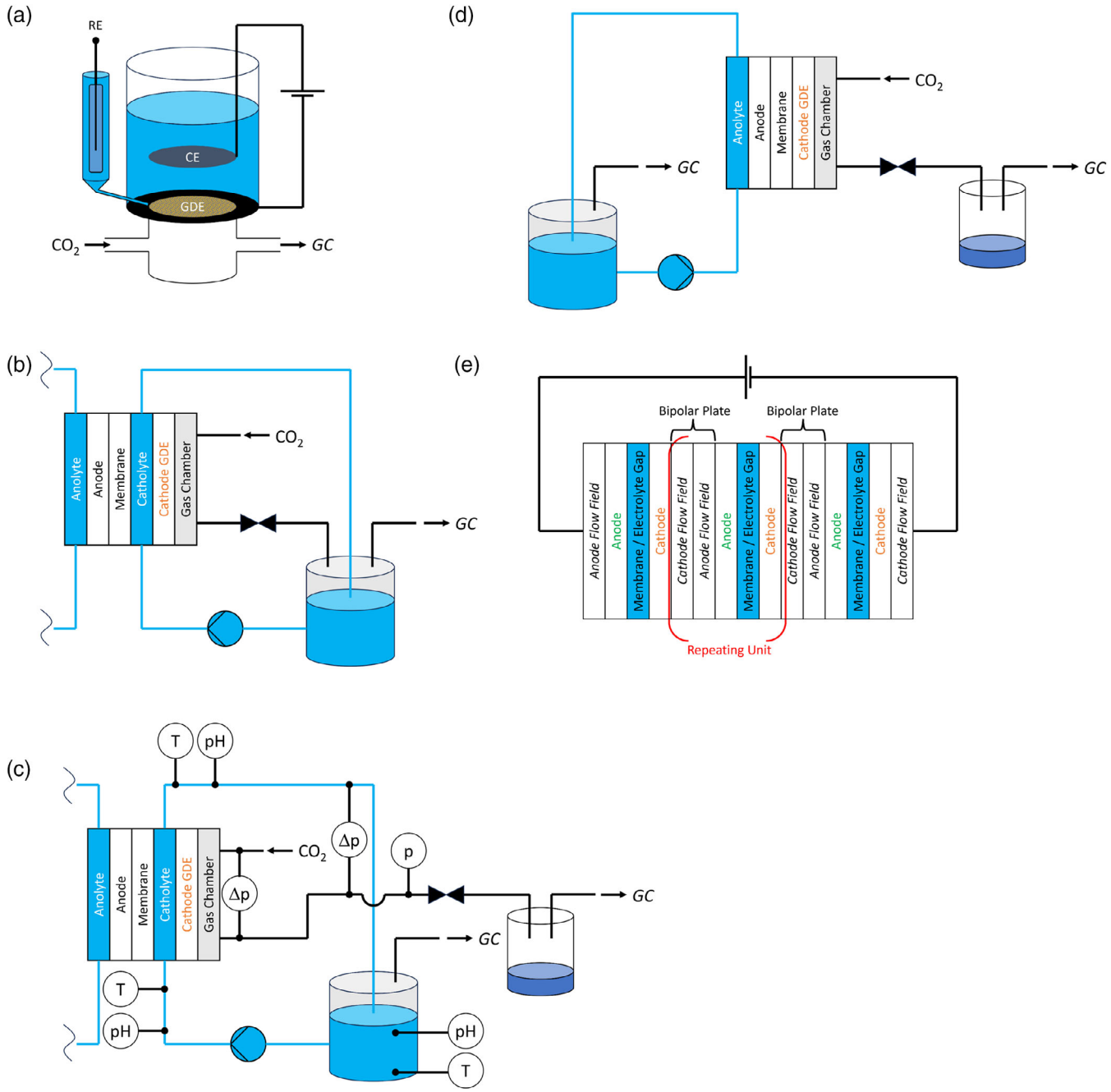

FIGURE 1 | (a) Half-cell for GDE testing in zero-gap configuration [15] and (b) common GDE flow cell setup [2]. Data are obtained from the potentiostat and the mixed product gases from both sides of the GDE. (c) GDE flow cell setup with enhanced environment data recording [18]. Product gas from both sides of the cathode is analyzed separately. In addition to potentiostat data, the absolute pressure, differential pressure, pH, and temperature are recorded at several points in the periphery. (d) Common MEA setup. Zero-gap anode and GDE are directly mounted on the membrane and supplied with their respective reagents from the backside. (e) Schematic representation of the functional layers in a cell stack. The bipolar plate is functionally the sum of the anode and cathode flow fields of two adjacent cells. A single cell forms a repeating unit in a stack.

researchers focus their attention on these electrodes and work to optimize their structure [1, 2] and understand the processes within the electrode [10]. Especially, the latter required the ability to operate these electrodes under defined and reproducible conditions, promoting the development of simple and elegantly designed GDE test cells [11]. Performance testing of new GDE designs, on the other hand, is typically conducted in flow cells, where the electrolytes are also continuous media streams [12]. Due to the importance of the GDE, the indicators for reporting the performance of CO_2 reduction reactions (CO_2RR) are usually largely determined and indicative of the performance of the GDE and the catalyst. The Faraday efficiency (FE) indicates the selectivity with which the electric current drives the formation of the desired products. Since its definition is independent of the cell or electrode type, it can be used to report the selectivity in catalyst characterization experiments in static cells as well as in performance tests using GDEs. While the FE is universal by its definition, the influence factors on the FE are highly dependent

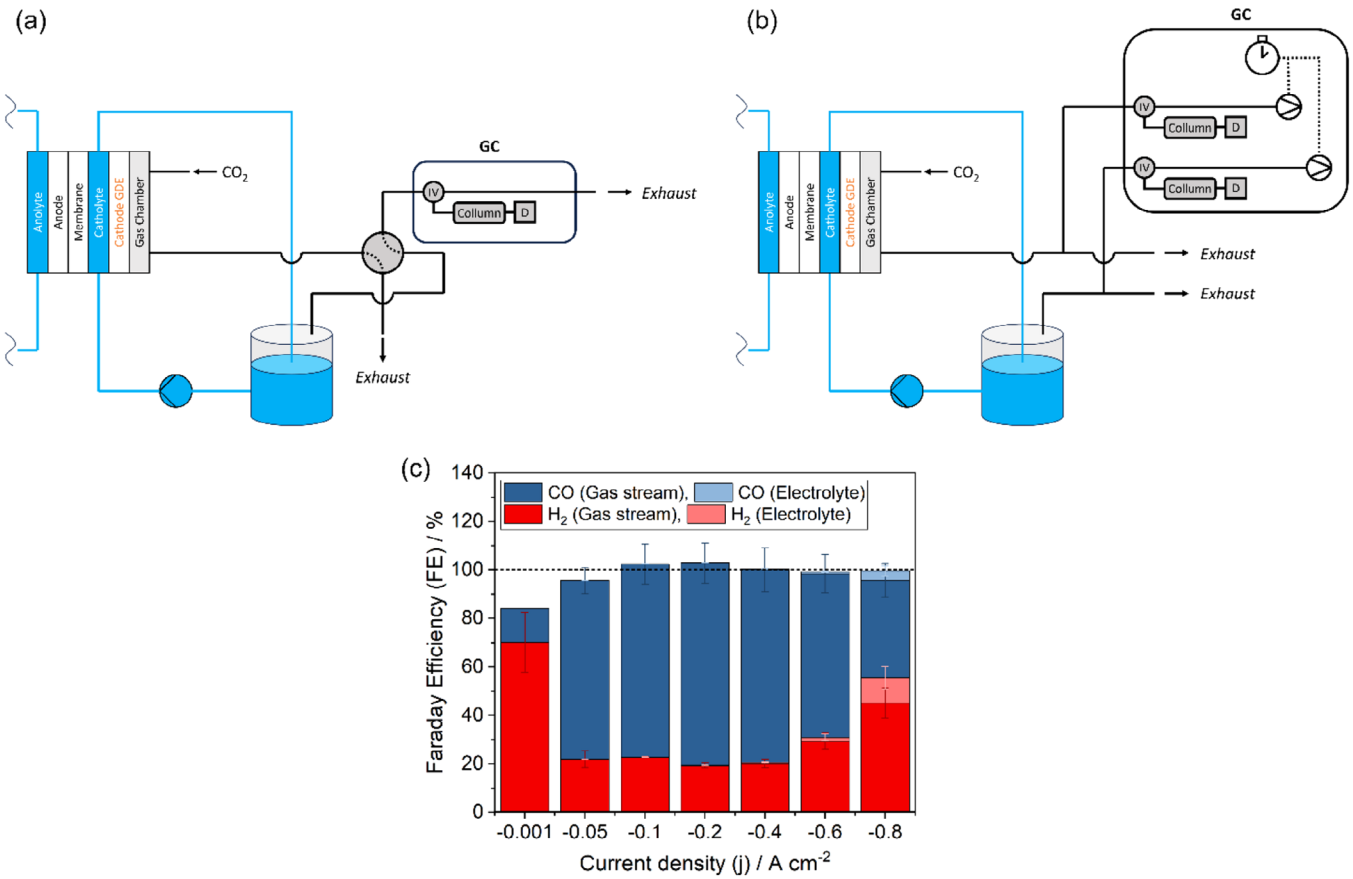

FIGURE 2 | Connection of a GC to a GDE flow cell (IV = Injection Valve, D = Detector). (a) Alternating measurement of gas from product gas side and electrolyte side with inline sample loop injection method. (b) Simultaneous measurement of gas from product gas side and electrolyte side with time-controlled extractive injection method. (c) Exemplary closed process balance for a GDE flow cell screening at stepwise increased current density with a constant CO_2/electron feed rate (Faraday Efficiency approx. 100%).

on the specific experiment and test environment (e.g., test in H-cell *vs.* GDE flow cell *vs.* MEA) [13]. When studying more complex systems like GDEs, the dependence between the FE and the applied potential or current can be a superposition of several factors [14]. The selectivity may be altered by the selectivity of the catalyst itself, by the transport of gases through the electrode and the liquid boundary, or by liquid ingress into the electrode, known as flooding [1, 10]. Understanding these dependencies requires careful experiment design with a broader focus than just the electrode, as the additionally collected data may be vital to determine the actual cause for a measured change in selectivity. CO_2RR studies are conducted using a variety of experimental strategies and test cells, depending on the focus and scope of the reported performance indicators. As a most extreme example, energy efficiency, on the other hand, is rarely reported unless the cell and the experiment were specifically optimized for it. Figure 2a–c show various cells for characterizing the performance of GDEs. Large static electrolyte vessels provide stable and well-defined conditions for short experiments, voltammetry, or impedance spectroscopy. In addition, the GDE surface can be easily accessed by Haber-Luggin capillaries for accurate potential measurement. Figure 1a may represent a fuel cell–derived GDE test cell published by [11, 15] or the FlexCell sold by Gaskatel and employed for CO_2 reduction [16]. Flow cells (e.g., Figure 1c) [2], on the other hand, are a closer representation of the application and can operate at commercially relevant current densities for extended periods of time. However, this requires the electrolyte gaps to be quite narrow, <3 mm [17-19], which interferes with accurate potential measurements due to non-ideal reference electrode placement. In such flow cells, the dynamic influence of the reaction on the cell environment is observed as the difference between the input and output streams. We, therefore, conducted experimental studies where the GDE was kept constant, and the features of the cell and the experimental conditions were varied to identify additional influence factors on the FE beyond the electric load, gas excess, and electrolyte composition [17, 18, 20]. For these experiments, the cell and periphery were designed to allow the integration of inline sensors and a separate analysis of the two product gas streams from either side of the GDE [17, 18] (Figure 1c). In contrast, it is common practice to mix the product gases collected from both sides of the GDE (Figure 1b) [2] by passing them through the headspace of the electrolyte vessel and to analyze a single gas stream to calculate the FE.

In addition to GDE flow cells, MEA flow cells are promising for application. In these cells, the membrane functions as an electrolyte between the anode and the cathode, rather than as an ion-selective separator. This allows for the use of only two chambers and reduces the electrode distance to tens of micrometers. Consequently, MEA cells can operate continuously at lower voltages and achieve higher energy efficiency than GDE flow cells. However, the membrane must also act as an alkaline

buffer layer on the cathode, calling for the use of anion exchange membranes or forward-biased bipolar membranes. AEM usage results in a loss of CO_2 into the anode compartment [21], which can be monitored by anode gas analysis, while the use of forward-biased bipolar membranes requires high operating pressure [22]. Comparing the operation and function of GDEs in both flow cell and MEA cell types is interesting with respect to their different designs. In a GDE flow cell, the GDE should release product gases into the gas chamber to prevent bubbles in the electrolyte. For MEA operation, this is not required, but the GDE catalyst layer is not cooled by a liquid stream, imposing a thermal conductivity requirement on the GDE and the membrane. To deliberately study the functions and influence of this element as well as its impact on the functions of others, we designed the cell to allow easy exchange of functional units. This abstract view of a cell stack is presented in Figure 1d. We, therefore, chose a layered flow cell to create modular cell designs and used this to our advantage when studying the impact of cell design features and stacking cells for both GDE flow cells and MEAs.

3 | Benefits of Synchronous Product Gas Analysis With Time-Controlled Extractive Sampling

CO_2 electroreduction on a GDE or an MEA involves species transport across the plane of the GDE or membrane. Therefore, complete process mass balancing requires data from both sides of these components. In our studies, we optimized gas analysis methods to consistently balance both sides of a GDE or an MEA. Gas chromatography (GC) is the most common method for gas analysis in CO_2RR. Samples are fed through sample loops in the GC, from which they get injected, separated, and analyzed using, e.g., thermal conductivity detectors (TCDs) (Figure 2a). Sample analysis typically takes 10 min. To gather data from either side of the GDE or MEA, a switching valve can alternate the gas feed through the GC.

While this method is generally expedient, we introduced two improvements. First, we used online GCs with two identical sets of columns and detectors on two inlets, allowing simultaneous, parallel analysis of two gas streams. Additionally, the GC was equipped with a time-controlled sampling pump to extract a sample from the product gas stream at a precise time just before injection (Figure 2b). Simultaneous analysis of products from both sides of an MEA or a GDE with a well-defined sampling period significantly improved data consistency and doubled the data point density per hour. All data in this study were obtained using this method, which we highly recommend. An example data set obtained for GDE flow cell screening at stepwise increased current density [18] is shown in Figure 2c.

4 | Operating Regimes of a GDE Flow Cell

It is important to determine the window in which a cell can be operated without accelerated GDE degradation. We define steady-state electrolyzer operation by every process parameter stabilizing at a consistent level for a specific current density, irrespective of previously applied currents. This stabilization converges to a dynamic level: some processes shift the cell environment from its thermodynamic equilibrium, while others work to compensate for these effects, achieving overall balance. Recently, we demonstrated a method to determine the operating regimes of GDE flow cells *via* chrono-potentiometric screening [18]. With the integration of sensors for precise monitoring of the electrode environment and process variables, new indicators that sufficiently describe the operating state of a GDE flow cell system have emerged. For example, the indicator j_{AD}, which stands for the transition current density from a steady state to an unstable process condition, can be determined simply by evaluating electrochemical data such as FE and applied current density [23]. Figure 3 shows that three GDE operating regimes can be distinguished by plotting the CO-specific current density against the total current density applied to a cell. If the slope of the j_{CO} graph is positive, the system is in a reversible operation regime. If, on the other hand, the slope of j_{CO} flattens out and reaches its peak, this represents the transition to unstable system states, which leads to irreversible damage to the electrode. Randomization of the sequence of applied current steps confirms j_{AD} as the limiting current density for the steady-state range, in which the electrode performance does not depend on the history of applied current densities. If current densities exceeding both the stable and the unstable operating range of the process are applied to a cell, only erratic process data oscillating between electrical voltage extremes and data noise are obtained. Microscopic *postmortem* examination of used electrodes showed no apparent signs of degradation after passing an electrochemical screening from 0.01 to 1 A cm^{-2}. From this observation, we conclude that the CO_2-reducing GDE is not the sole constraint of such a process but that the cell reactor itself runs into current density limitations as a result of the reaction environment evolution driven by specific cell designs. We have analyzed these phenomena and explored the possibilities of increasing the maximum applicable current density hereafter. Dynamic operation with minimal degradation and consistently high CO_2 conversion selectivity will be essential for the applications of CO_2 electrolysis in the future [24].

5 | Current-Dependent Changes in the GDE Flow Cell Environment

As the current density increases, reduction processes at the electrode surface intensify. Consequently, practically all process environment variables of a GDE directly or implicitly depend on the applied current density. Changes in the electrode environment were recorded by integrating a range of analytical sensors in the reactor system to monitor process variables such as the electrolyte temperature or the relative pressures occurring in the system around the GDE. It was possible to analyze variations in these variables until a process limit was reached [18]. With increased reaction rates, the electrodes release a large amount of reaction heat to the liquid electrolyte medium in the electrolyte gap at high current densities. Due to the small electrolyte volume in the gap, the electrolyte heats up considerably, and dissolved gases are released from the liquid medium in the form of bubbles within the gap. When a specific temperature and pressure are reached in the electrolyte gap, water evaporation begins to occur and contributes to the formation of gas bubbles in the electrolyte gap. For the abovementioned reasons, the pressure on the liquid side of a GDE increases steadily with increasing current density. The total voltage required for cell operation increases along with the increasing gas content in the electrolyte gap. Once the

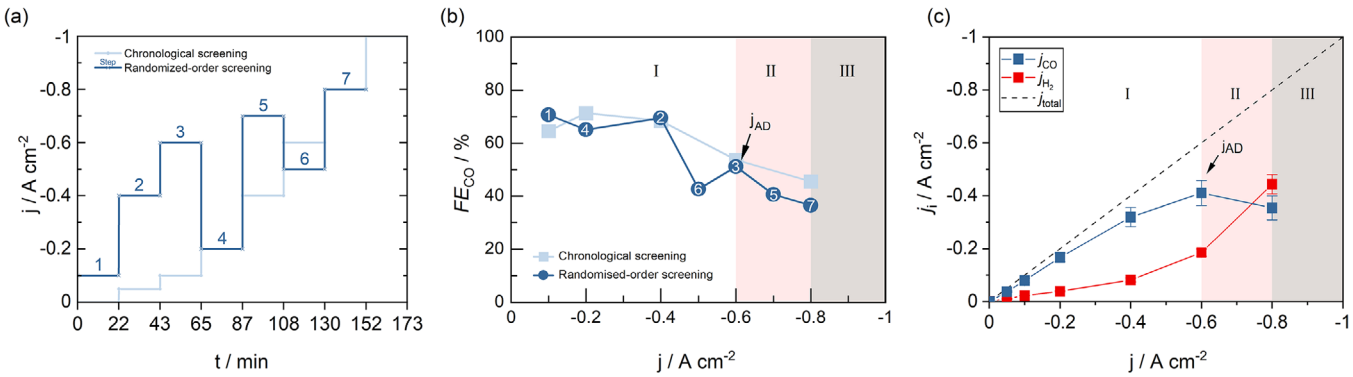

FIGURE 3 | Validation of a chrono-potentiometric screening method to experimentally determine the range of steady-state GDE operation. (a) Order of applied current density steps for both a chronological staircase screening protocol and a randomized-order experiment with shuffled current density loads, (b) corresponding CO-Faraday efficiencies recorded for GDEs tested in chronological and shuffled current density orders, and (c) product-specific current density in case of a chronological staircase screening. GDE states of operation are marked as (I) steady-state operation, (II) states of accelerated GDE degradation, and (III) inaccessible states. The transition point of GDE steady-state operation to unstable states is indicated by j_{AD}, the transition current density to states of accelerated GDE degradation, reproduced from Martens *et al.* [18] with permission from the Royal Society of Chemistry.

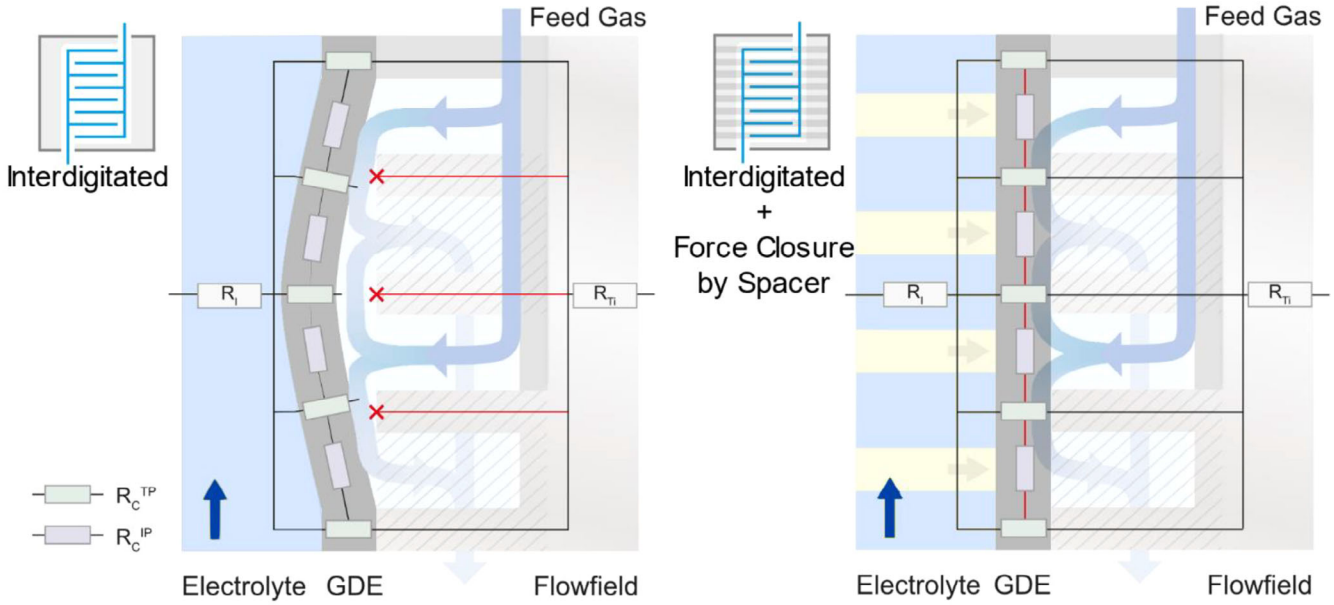

FIGURE 4 | Schematic illustration of the electrical resistances of the titanium flow field (RTI), the GDE in-plane resistance (RCIP), the GDE through plane resistance (RCTP), the ionic resistance of the electrolyte (RI), and the behavior of the GDE on the interdigitated flow field. (Left) Pressure generated by feed gas in the interdigitated flow field pushes the GDE towards the electrolyte and decreases the GDE-current collector contact area; the electrical current path is forced through the in-plane area of the GDE. (Right) Force, induced by a spacer, pushes the GDE onto the interdigitated flow field, electrical current can pass along the flow field. Adapted version from Quentmeier *et al.* [17].

liquid-to-gas flow ratio in the electrolyte gap becomes disproportionately high, the ion exchange in the electrolyte gap is significantly obstructed, and current can no longer pass through the cell in a controlled manner. Operating a cell in flow-through CO_2 supply mode can be an additional source of CO_2 gas in the catholyte gap [25]. This issue may especially be encountered when supplying electrolyzers at high current densities with proportionally high CO_2 feed flows for high conversion rates. When CO_2 bubbles spill into the electrolyte gap, they become unavailable for catalytic reduction. Controlling high gas flow may be achieved by adjusting the resistance in exhaust lines, which alters the apparent correlation of CO_2 gas pressure and current density while maintaining a constant CO_2-to-electron supply rate [18, 26]. With the introduction of an active cooling system for external electrolyte reservoirs and by increasing the electrolyte conductivity through the selection of higher concentrated electrolyte solutions, the maximum current density range at which a GDE flow cell with liquid electrolyte can be operated on a laboratory scale (10 cm^2 active GDE area) can be increased to 1 A cm^{-2} and more.

6 | Functions of Media Flow Compartments for GDE Flow Cell Operation

The continuous operation of a flow cell requires a constant delivery of gaseous educt and constant removal of product to and from the electro-catalytically active sites of the GDE. This function is usually served by flow fields that are placed on the rear side of the GDE. The current collector functions as a stabilizing structure and provides electric contact to the GDE, which can be an open frame or a backing plate with a flow field carved into it [27]. From the nature of this design, a trade-off can be derived between the current collector contact area to the GDE and the contact area of the gas to the GDE. Thus, the functions of the current collector and the functions of the flow field are interdependent. In a recent study, we have linked the trade-off described to the performance indicators, cell voltage and FE of a GDE flow cell. We demonstrated that a large GDE gas contact area leads to high FE and high cell voltages, while the opposite effect was observed for a large GDE-current collector contact area. We introduced an interdigitated flow field that mitigates the trade-off by forcing the gas through the GDE (Figure 4), yielding higher FE even with a reduced CO_2 supply [17]. However, the benefits of this flow-field design can only be exploited when fixing the GDE's position in the flow cell. The mechanical stability of the GDE is limited, and forcing the gas through the GDE leads to a bending of the GDE and a loss of contact with the current collector. It becomes evident that the function of the current collector depends on the forced closure in the cell and, therefore, on the mechanical stability of the electrolyte gap. Since the electrolyte gap in a GDE flow cell does not provide mechanical support to fix the GDE's position on the current collector, a spacer needs to be implemented. Implementing structures in electrolyte gaps is associated with certain challenges, such as the increase in pressure drop and the creation of non-conductive areas *via* the non-conductive characteristics of the spacer or by the trapping of gas bubbles. Therefore, we introduced an ionically conductive spacer in the electrolyte gap, which provides the necessary structure to fix the GDE at its position and reduces bubble-induced noise by bridging the gas bubbles in the electrolyte gap. We emphasize that the modification of media flow compartments, as demonstrated in our recent work, is necessary to fulfill prerequisites for stacking the flow cells and thus scaling the process [17].

7 | Impact of Stacking on the Behavior of an MEA Cell

In the field of electrolysis, the stacking of flow cells is a common practice for scaling processes. In contrast to scaling by increasing the active area of the electrolyzers, the voltage increases proportionally to the number of cells instead of the applied current. Thus, the increase in ohmic losses in the periphery is mitigated in the scaling process [8].

Regarding the operation of electrolyzer stacks, a different behavior of the individual cells in the stack needs to be considered in comparison to the equivalent single cell. Stack-related effects such as shunt currents, media flow distribution, or temperature development cannot be derived from investigations of a single cell. Therefore, we recently introduced a modular short-stack design with MEAs and compared the behavior of a three-cell stack with MEAs to the equivalent single cell at various current densities. While the short stack replicates the performance of its individual single-cell counterpart at current densities ranging from 100 to 200 mA cm^{-2}, the short stack surpasses the single cell's performance at higher current densities (300–400 mA cm^{-2}) by operating at lower stack voltages. We demonstrated that the reduced stack voltage originates from higher temperatures in the short stack, which enhanced the ionic conductivity of the membrane as well as the charge transfer of the reactions at the electrodes [20]. Aside from the temperature increase, we observed the formation of temperature gradients in the stack, which became evident through voltage differences between the individual cells. The function of heat dissipation is served by the electrolyte, the cooling in a cell with an MEA is only managed by the anolyte [20]. In contrast to the single cell, the cells in the stack are additionally cooled by the anolyte of the neighboring cell. However, due to the asymmetry of the cells, the cell providing the terminal cathode is the only cell that truly replicates the single cell and does not incorporate the additional cooling. Thus, higher temperatures can be expected in the cell, providing the terminal cathode, leading to lower cell voltages. By exploiting the modularity of our stack design, we created a more symmetric stack with an additional cooling chamber providing the same environment to all individual cells. This modified stack operated with a more evenly distributed voltage. Only minor differences in voltage were observed that showed characteristics of shunt current formation, which was subsequently investigated, and the influence was found to be negligible [20].

8 | Conclusions

To optimize CO_2 reduction reaction (CO_2RR) technology for application readiness, it is imperative to fully understand which functions are fulfilled by each component of an electrolyzer and how the processes and conditions in the cell are coupled. Fully understanding the functions of the gas flow field requires systematically changing both the gas flow field and the spacer in the electrolyte gap, showing that in CO_2RR, the entire cell and its periphery have to be analyzed as a whole. If cell components like electrolyte gaps are omitted or combined differently, their individual functions, such as force closure or heat removal, shift to other cell parts and interdependencies may change. We have demonstrated how challenges associated with such changes can be tackled by systematic experiments and cell design. Achieving comparability in GDE characterization is dependent on the definition of the impact and functions of the other cell components and the current-driven changes in the cell environment. Parameter variation in a single experiment to screen conditions or assess dynamic operation requires operating the GDE within a controlled window where the convergence of cell conditions is ensured. Monitoring the conditions in the periphery at the cell inlet and outlet is key to tracking changes in the cell, as well as the interaction of the GDE and the cell or multiple cells in a stack. We demonstrated how expanding the scope of data collection and the arrangement of experimental steps can make new information on the system accessible. We recommend expanding the data discussed in the field of electrochemical CO_2 reduction beyond FE and energy efficiency and the properties of the employed materials.

9 | Outlook

Our approach for improving experimental strategies may be particularly beneficial when scaling up or optimizing operation windows *via* a 'Design of Experiments' (DOE) approach. Scaling distinct functional modules in defined directions while tracking the conditions in the cell and periphery is vital to determining the scale dependencies of cell properties and processes. Overdetermination of the parameter space and ill-defined variation ranges in a DOE can be avoided using our approach of identifying steady-state regimes and interdependencies of process parameters. A more accurate description of the state of operation may also improve the comparability of catalyst performance in different cell or electrode types.

Acknowledgements

The authors kindly acknowledge funding by the Federal Ministry of Education and Research (BMBF), Project: iNEW2.0 'Inkubator Nachhaltige Elektrochemie', funding code: 03SF0627A. The authors thank Sebastian B. C. Lehmann for his contributions to graphical designs.

Conflicts of Interest

The authors declare no conflicts of interest.

Data Availability Statement

The data that support the findings of this study are available from the corresponding authors upon reasonable request.

References

1. S. Garg, M. Li, A. Z. Weber, et al., "Advances and Challenges in Electrochemical CO_2 Reduction Processes: An Engineering and Design Perspective Looking Beyond New Catalyst Materials," *Journal of Materials Chemistry A* 8 (2020): 1511–1544.

2. L. M. Baumgartner, A. Goryachev, C. I. Koopman, et al., "Electrowetting Limits Electrochemical CO_2 Reduction in Carbon-Free Gas Diffusion Electrodes," *Energy Advances* 2 (2023): 1893–1904.

3. T. N. Nguyen and C.-T. Dinh, "Gas Diffusion Electrode Design for Electrochemical Carbon Dioxide Reduction," *Chemical Society Reviews* 49 (2020): 7488–7504.

4. S. Nitopi, E. Bertheussen, S. B. Scott, et al., "Progress and Perspectives of Electrochemical CO_2 Reduction on Copper in Aqueous Electrolyte," *Chemical Reviews* 119, no. 12 (2019): 7610–7672.

5. K. Yang, R. Kas, W. A. Smith, and T. Burdyny, "Role of the Carbon-Based Gas Diffusion Layer on Flooding in a Gas Diffusion Electrode Cell for Electrochemical CO_2 Reduction," *ACS Energy Letters* 6, no. 1 (2021): 33–40.

6. L. M. Baumgartner, C. I. Koopman, A. Forner-Cuenca, and D. A. Vermaas, "When Flooding Is Not Catastrophic—Woven Gas Diffusion Electrodes Enable Stable CO_2 Electrolysis," *ACS Applied Energy Materials* 5 (2022): 15125–15135.

7. J.-B. Vennekötter, T. Scheuermann, R. Sengpiel, and M. Wessling, "The Electrolyte Matters: Stable Systems for High Rate Electrochemical CO_2 Reduction," *The Journal of CO_2 Utilization* 32 (2019): 202–213.

8. B. Endrődi, E. Kecsenovity, A. Samu, et al., "Multilayer Electrolyzer Stack Converts Carbon Dioxide to Gas Products at High Pressure With High Efficiency," *ACS Energy Letters* 4 (2019): 1770–1777.

9. D. Higgins, C. Hahn, C. Xiang, T. F. Jaramillo, and A. Z. Weber, "Gas-Diffusion Electrodes for Carbon Dioxide Reduction: A New Paradigm," *ACS Energy Letters* 4, no. 1 (2019): 317–324.

10. N. T. Nesbitt, T. Burdyny, H. Simonson, et al., "Liquid–Solid Boundaries Dominate Activity of CO_2 Reduction on Gas-Diffusion Electrodes," *ACS Catalysis* 10, no. 23 (2020): 14093–14106.

11. S. Alinejad, J. Quinson, Y. Li, et al., "Optimizing the Use of a Gas Diffusion Electrode Setup for CO_2 Electrolysis Imitating a Zero-Gap MEA Design," *Journal of Catalysis* 429 (2024): 115209.

12. D. M. Weekes, D. A. Salvatore, A. Reyes, A. Huang, and C. P. Berlinguette, "Electrolytic CO_2 Reduction in a Flow Cell," *Accounts of Chemical Research* 51 (2018): 910–918.

13. S. Alinejad, J. Quinson, G. K. H. Wiberg, et al., "Electrochemical Reduction of CO_2 on Au Electrocatalysts in a Zero-Gap, Half-Cell Gas Diffusion Electrode Setup: A Systematic Performance Evaluation and Comparison to an H-Cell Setup," *ChemElectroChem* 9 (2022): e202200341.

14. J.-B. Vennekoetter, R. Sengpiel, and M. Wessling, "Beyond the Catalyst: How Electrode and Reactor Design Determine the Product Spectrum During Electrochemical CO_2 Reduction," *Journal of Chemical Engineering* 364 (2019): 89–101.

15. D. Zhang, J. Du, J. Quinson, and M. Arenz, "On the Electro-Oxidation of Small Organic Molecules: Towards a Fuel Cell Catalyst Testing Platform Based on Gas Diffusion Electrode Setups," *Journal of Power Sources* 522 (2022): 230979.

16. P. Lesnicenoks, A. Knoks, S. Piskunov, L. Jekabsons, and J. Kleperis, "N-Graphene Sheet Stacks/Cu Electrocatalyst for CO_2 Reduction to Ethylene," *Electrochem* 3 (2022): 229–238.

17. M. Quentmeier, B. Schmid, H. Tempel, H. Kungl, and R.-A. Eichel, "Toward a Stackable CO_2-to-CO Electrolyzer Cell Design—Impact of Media Flow Optimization," *ACS Sustainable Chemistry & Engineering* 11 (2023): 679–688.

18. C. Martens, B. Schmid, H. Tempel, and R.-A. Eichel, "CO_2 Flow Electrolysis—Limiting Impact of Heat and Gas Evolution in the Electrolyte Gap on Current Density," *Green Chemistry* 25 (2023): 7794–7806.

19. J. E. Huang, F. Li, A. Ozden, et al., "CO_2 Electrolysis to Multicarbon Products in Strong Acid," *Science* 372 (2021): 1074–1078.

20. M. Quentmeier, B. Schmid, H. Tempel, and R.-A. Eichel, "Modular CO_2-to-CO Electrolysis Short-Stack Design—Impact of Temperature Gradients and Insights Into Position-Dependent Cell Behavior," *ACS Sustainable Chemistry & Engineering* 12 (2024): 3876–3885.

21. Z. Liu, H. Yang, R. Kutz, and R. I. Masel, "CO_2 Electrolysis to CO and O_2 at High Selectivity, Stability and Efficiency Using Sustainion Membranes," *Journal of the Electrochemical Society* 165 (2018): J3371–J3377.

22. K. Pellumbi, D. Krisch, C. Rettenmaier, et al., "Pushing the Ag-Loading of CO_2 Electrolyzers to the Minimum via Molecularly Tuned Environments," *Cell Reports Physical Science* 4 (2023): 101746.

23. Y. Gu, J. Wei, X. Wu, and X. Liu, "A Study on Improving the Current Density Performances of CO_2 Electrolysers," *Scientific Reports* 11 (2021): 11136.

24. B. M. Fekete, M. Bacskó, J. Zhang, and M. Chen, "Storage Requirements to Mitigate Intermittent Renewable Energy Sources: Analysis for the US Northeast," *Frontiers in Environmental Science* 11 (2023): 1076830.

25. M. Duarte, B. De Mot, J. Hereijgers, and T. Breugelmans, "Electrochemical Reduction of CO_2: Effect of Convective CO_2 Supply in Gas Diffusion Electrodes," *ChemElectroChem* 6 (2019): 5596–5602.

26. T. Haas, R. Krause, R. Weber, M. Demler, and G. Schmid, "Technical Photosynthesis Involving CO_2 Electrolysis and Fermentation," *Nature Catalysis* 1 (2018): 32–39.

27. H. Teuku, I. Alshami, J. Goh, M. S. Masdar, and K. S. Loh, "Review on Bipolar Plates for Low-Temperature Polymer Electrolyte Membrane Water Electrolyzer," *International Journal of Energy Research* 45 (2021): 20583–20600.